https://doi.org/10.5194/egusphere-2025-2493
Preprint. Discussion started: 17 June 2025

Balancing water column and sedimentary ^{234}Th fluxes to quantify coastal marine carbon export

Madeline G. Healey[1], Erin E. Black[2], Christopher K. Algar[1], Maria Armstrong[1], Stephanie S. Kienast[1]

[1] Department of Oceanography, Dalhousie University, Halifax, Nova Scotia, Canada
[2] Department of Earth and Environment, University of Rochester, Rochester, New York, USA

Correspondence to: Madeline G. Healey (mhealey@dal.ca)

Abstract. Quantitative estimates of particulate organic carbon (POC) flux and burial in coastal systems are critical for constraining coastal carbon budgets and understanding their role in regional and global carbon cycling. In this study, POC export fluxes were quantified in the Bedford Basin, a coastal inlet in the Northwest Atlantic, based on measurements of ^{234}Th/^{238}U disequilibria and the POC:^{234}Th ratio on small (1-51 µm) and large (> 51 µm) particles. These water column export fluxes were compared to sediment accumulation fluxes of ^{234}Th and POC to refine the carbon budget in the Bedford Basin. The coupled water column-surficial sediment sampling approach, which is relatively new, was applied quasi-seasonally throughout 2021 – 2024, including for the first time in boreal winter. Total ^{234}Th activities reveal persistent deficits with respect to ^{238}U throughout the water column, likely due to extensive particle scavenging, which is also indicated by high ^{234}Th activities on particles. Here, we find that the removal of ^{234}Th in the water column is typically balanced, within uncertainties, by the inventory of excess ^{234}Th in underlaying marine sediments. This finding reveals that on the timescale of ~100 days, the ^{234}Th budget in the Bedford Basin is in balance, and no major particle loss is occurring. Using the POC:^{234}Th ratio on sinking particles and integrated ^{234}Th water column fluxes, we report a mean (± s.d.) depositional flux of 20 ± 14 mmol C m^{-2} d^{-1} (range 3.6 to 44.5 mmol C m^{-2} d^{-1}) to the seafloor. This mean flux translates to an annual molar flux of 7.2 ± 0.7 mol C m^{-2} yr^{-1}, within a factor of 2 to model estimates and previous sediment trap results at this site. Our findings contribute to ongoing research efforts in the Bedford Basin, and aid in the evaluation of coastal regions in local carbon budgets.

1. Introduction

Coastal and continental shelf zones represent only ~ 7 – 10% of the global ocean surface area but host up to 30% of global marine primary production (Muller-Karger et al., 2005) and are important for the long-term burial of organic matter. Coastal areas are dynamic transition zones between land and ocean, where biogeochemical processes modify carbon cycling. In turn, these processes influence air-sea carbon dioxide (CO_2) exchanges and thus exert a significant control on regional and global carbon cycles. A series of biologically mediated processes referred to as the biological carbon pump (BCP) are important in co-regulating atmospheric CO_2 concentrations. In the sunlit surface ocean, primary producers photosynthesize inorganic CO_2 into particulate organic carbon (POC) at a rate of ~ 50 Pg C yr^{-1} (Longhurst et al., 1995). A portion of this POC leaves the surface ocean and sinks to depth, whereby a small fraction ends up sequestered in marine sediments. The traditional method of estimating sinking POC fluxes is based on sediment traps, which suffer from conveyance issues and hydrodynamic biases (Butman, 1986). Additionally, living organisms ("swimmers") can enter traps and bias particle flux estimates, an issue which is more severe in the shallow waters characterizing coastal and shelf areas compared to the open ocean (Buesseler et al., 2007). Given these methodological constraints, the confluence

https://doi.org/10.5194/egusphere-2025-2493
Preprint. Discussion started: 17 June 2025

of terrestrial and marine carbon sources, and temporal and spatial heterogeneity, the processes controlling carbon cycling in coastal and shelf regions remain elusive.

First proposed by Bhat et al. (1969), the disequilibrium between the naturally occurring radioisotopes thorium-234 (^{234}Th, $t_{1/2}$ = 24.1 d) and uranium-238 (^{238}U, $t_{1/2}$ = 4.47 x 10^9 yr) is commonly measured to quantify sinking fluxes of carbon and other elements in the ocean. In shallow regions, the removal of ^{234}Th from the water column results in an excess of ^{234}Th ($^{234}Th_{xs}$) on the seafloor in marine sediments (Aller and Cochran, 1976), offering a unique opportunity to explore one-dimensional (1D) particle dynamics and export. A recent global oceanic compilation identified 223 studies that applied the ^{234}Th/^{238}U disequilibrium method, encompassing a total of 1981 unique stations (Ceballos-Romero et al. 2022). However, in nearshore coastal settings, defined here as within 5 nautical miles (nm) of the coast, there are comparatively fewer studies. Of the 1981 unique stations that have been sampled for ^{234}Th (Ceballos-Romero et al. 2022), only 1.4% are in nearshore coastal settings. Importantly, only four of the 223 studies make coupled, quasi-simultaneous measurements of the ^{234}Th deficit in the water column and the expected excess of ^{234}Th in surficial sediments (Cochran et al., 1995; Charette et al. 2001; Black et al., 2023, Lepore et al., 2007). By using this approach, detailed insights into carbon export can be made that aid in carbon budget evaluations. This study applies the coupled water column-sediment approach to evaluate both ^{234}Th and POC sinking fluxes and their respective sediment accumulation fluxes in the Bedford Basin, a coastal fjord in the Northwest Atlantic Ocean.

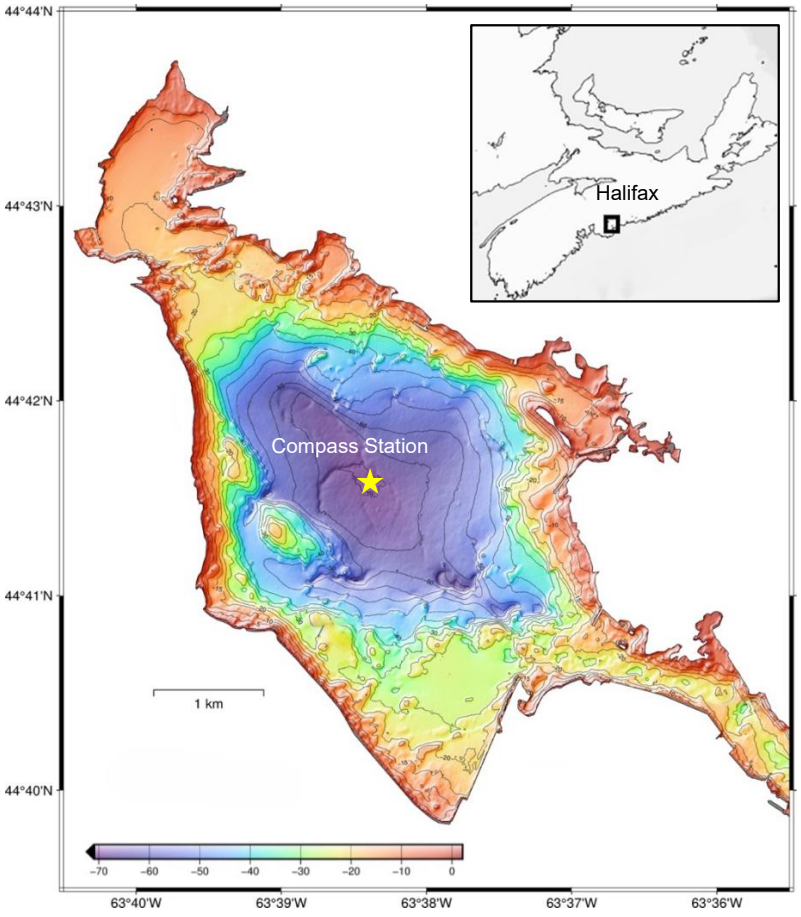

https://doi.org/10.5194/egusphere-2025-2493
Preprint. Discussion started: 17 June 2025

Figure 1. A bathymetric map of the Bedford Basin (GEBCO Gridded Bathymetry Data). The Compass Buoy Station (70 m), the main sampling location, is represented by the yellow star. The inset map (upper right corner) shows the Bedford Basin in Halifax, Nova Scotia, Atlantic Canada.

2. Methods

2.1 Study Site

The Bedford Basin (BB; 44.6955° N, 63.6330° W; Fig. 1) is a 17 km^2, semi-enclosed fjord in Nova Scotia, Canada, and forms the northwestern part of the Halifax Harbour. The basin has a volume of 5.6 x 10^8 m^3 (Burt et al., 2013) and a maximum depth of 70 m. It is connected to the inner Halifax Harbour via a 20 m deep sill and to the open Atlantic Ocean by a 10 km long, 400 m wide channel. Runoff from the Sackville River (1.5 × 10^8 m^3 yr^{-1}, Kepkay et al., 1997) and surrounding areas is discharged into the basin, creating a two-layer estuarine circulation – a fresher top layer and a denser bottom layer from the shelf water intruding from the entrance of the Halifax Harbour. The hydrography of the basin is characterized by annual cycles of winter mixing and summer stratification. Stratification is established in the spring (April – May) and persists into the fall and winter (November – February). In most years, the water column fully mixes during the late winter (mid-February to mid-March). Seasonal hypoxia occurs in the deeper basin during the fall-winter months, but re-oxygenation takes place during late winter mixing. In spring, a phytoplankton bloom typically occurs as surface stratification increases. Occasional intrusions of dense Scotian Shelf water can replenish either the bottom or mid-depth waters (Shi and Wallace, 2018; Haas et al., 2021). The Bedford Basin Monitoring Program (BBMP), established by the Bedford Institute of Oceanography (BIO) has conducted weekly measurements of water properties since 1992. Despite a large array of oceanographic variables that are frequently sampled by BBMP and other research initiatives, limited information exists on POC export and burial in this important urban coastal region.

2.2 Hydrographic Properties

Weekly monitoring at the Compass Buoy Station in the centre of the Bedford Basin provides temperature, salinity, oxygen- and chlorophyll concentrations (BBMP, Seabird CTD SBE-25). To capture the mean conditions near the basin floor, we derived mean values for temperature, salinity, and oxygen between 60 m water depth and the bottom (or the deepest available measurement). We then calculated the anomalies between consecutive profiles, resulting in a time series of anomalies that reflects changes from week to week in each variable in the deep basin (Fig. 2d).

2.3 Total ^{234}Th & ^{238}U activities in seawater

Total (dissolved + particulate) ^{234}Th ($^{234}Th_{tot}$) was measured six times at the Compass Station between 2021 – 2024. Water column samples were taken with Niskin bottles (10 L) at 9 discrete depths. After the addition of a ^{230}Th yield tracer, unfiltered sea water samples (2 L) were processed according to the MnO_2 co-precipitation technique (Pike et al., 2005). Following co-precipitation, samples were filtered onto quartz fiber filters (QMA, 25mm diameter, 1 µm nominal pore) following Cai et al (2006). After filtration, filters were dried (55° C), mounted on sample holders, covered with Mylar™ film (1 layer) and aluminium foil (2 layers), and their beta emissions were measured on low-level beta GM multi-counters (Risø National Laboratory, Denmark). Samples were counted until the error was typically < 3%. After ~ 120 days from collection (i.e., after 5 half-lives of ^{234}Th), samples were recounted to determine the non-^{234}Th beta activity stemming from other radionuclides included in the precipitate, which was subtracted from the first count. After final counting was completed, the chemical recovery of ^{230}Th

https://doi.org/10.5194/egusphere-2025-2493
Preprint. Discussion started: 17 June 2025

was determined by inductively coupled plasma mass spectrometry (ICP-MS) as outlined in Clevenger et al. (2021), yielding a mean recovery of 85 ± 12% (n = 63). The net counting rate was corrected for ^{234}Th decay and ingrowth, counting efficiency, and chemical recovery. The uncertainties in the $^{234}Th_{tot}$ activities are determined from counting statistics and the propagation of errors in relation to sample processing, including mass and volume measurements, and ICP-MS recovery analysis. The parent ^{238}U activity is derived from salinity following the relationship given by Owens et al (2011), (Eq. 1).

$$238U\ (\pm 0.047\ dpm\ L^{-1}) = (0.0786 \pm 0.045) \times Salinity - (0.315\ \pm 0.158) \quad (1)$$

Seawater ^{234}Th activities are used to calculate cumulative water column ^{234}Th fluxes (dpm m^{-2} d^{-1}) as follows:

$$Flux_{Th\ @\ z} = \int_0^z (\lambda_{Th}(238U - 234Th) + w\frac{\partial 234_{Th}}{\partial z} - u\frac{\partial 234_{Th}}{\partial x} - v\frac{\partial 234_{Th}}{\partial y})dz \quad (2)$$

Here, ^{234}Th is $^{234}Th_{tot}$ activity (dpm L^{-1}), ^{238}U is the salinity derived ^{238}U activity (dpm L^{-1}; Owens et al., 2011), λ_{Th} is the decay constant of ^{234}Th (0.0288 d^{-1}), w is the upwelling velocity, u is the zonal velocity, v is the meridional velocity, and the ∂ terms are the vertical (∂z), west to east (∂x), and south to north (∂y) gradients. Applying the 1D steady state model, Eq. 2 can be simplified to:

$$Flux_{Th\ @z} = \int_0^z \lambda_{Th}(^{238}U - {}^{234}Th)\,dz \quad (3)$$

Given the temporal resolution of this study, and the fact that ^{234}Th profiles were not measured during consecutive weeks – months but rather on a quasi-seasonal scale, the use of a non-steady-state model for ^{234}Th flux is not feasible, and we apply the steady state condition. The validity the 1D steady-state assumption is discussed further in Section 4.3. The uncertainties of the flux are the propagated measurement error.

2.4 Particulate ^{234}Th and POC in seawater

Size fractionated particulate ^{234}Th samples ($^{234}Th_p$) were collected by in-situ pumping of ~ 30 L at 3 depths (~20,40,60 m) using large volume pumps (McLane Laboratories™). Filter heads were equipped with a 51 µm pore size Nitex filter above a 1 µm pore size QMA filter (pre-combusted). The large particle material (> 51 µm) captured on the Nitex screens was rinsed onto QMA filters (1 µm pore size, 25 mm diameter, pre-combusted) using filtered and UV treated seawater. The small particulate material (1 - 51 µm) captured on the QMA filter was subsampled by cutting out a 25 mm diameter 'punch'. After drying (55°C) all particulate samples were mounted onto sample holders and analyzed on beta counters (see above). Following the second counting, particulate samples were prepared for POC measurement by fumigation under HCl vapor for 6 h inside a glass desiccator to remove the carbonate phase. Samples were dried at 50°C and packed into tin cups and then measured on an Elemental Analyzer (Elementar MicroCube & Isoprime 100). For each pump cast, an additional filter head was attached to deepest pump to obtain a seawater process blank ("dipped blank"; Lam et al., 2015). The dipped blanks were exposed to seawater for the same amount of time and processed as regular samples. Dipped blank filters were used as process blanks for blank subtraction, detection limit determination, and uncertainty calculations. For calculating POC fluxes, we assume that the POC:^{234}Th ratio on the large particle fraction (> 51 µm) is representative of the sinking flux and is calculated with Eq. 4. For comparison, the POC:^{234}Th ratio on the small particle fraction (1-51 µm) was also calculated using Eq. 4.

$$POC\ flux = Flux_{Th\ @\ z} * \left(\frac{\mathrm{POC}}{^{234}\mathrm{Th}}\right) \quad (4)$$

https://doi.org/10.5194/egusphere-2025-2493
Preprint. Discussion started: 17 June 2025

To investigate the role of resuspension in this study and in the Bedford Basin as a whole, the residual beta activity (i.e., after 5 half-lives) was analyzed. A novel resuspension proxy, the residual activity of particulate ^{234}Th (Ra_{P234}; Lin et al., 2016) has previously been applied to investigate particle dynamics in coastal sites. Briefly, the Ra_{P234} signal comes from "supported" radionuclides bound to particle components like biogenic or lithogenic materials. Terrigenous particles retain radionuclides such as ^{234}Th (from ^{238}U decay) and ^{212}Bi (from ^{228}Th decay), contributing to β counting due to their long half-lives. In contrast, "unsupported" ^{234}Th is adsorbed in the water column and is the focus of this (and other studies) using the ^{234}Th/^{238}U method to quantify carbon fluxes. The supported Ra_{P234} signal indicates sediment resuspension, potentially biasing particle flux measurements. The novel proxy of residual beta activity of ^{234}Th (Lin et al., 2016) was obtained from the second counting rates of ^{234}Th after 5 half-lives (~120 d) passed, and calculated as:

$$Ra_{p234} = \frac{n_{P2} - n_0}{\varepsilon V} \quad (5)$$

Where n_{p2} is the second β counting rate of particulate ^{234}Th (mean 0.3 cpm), n_0 is the blank mean (0.24 counts per minute, cpm), ε is the detector efficiency (0.3), and V is volume of seawater pumped (L). The detection method is defined here as two times the standard deviation of the blank and corresponds to 128.2 dpm m^{-3}.

2.5 Excess ^{234}Th inventories in seafloor sediments

For the measurement of ^{234}Th in the sediment, a KC Denmark™ Multicorer was deployed at the Compass Station following water column sampling. Once dry, sediments were manually homogenized and weighed into a petri-dish. Analysis of sedimentary ^{234}Th and ^{238}U activities were carried out by non-destructive gamma counting (Dartmouth College, USA). The raw ^{234}Th activities (at 63.3 keV) in sediments were decay corrected to time of collection. Unsupported or 'excess' ^{234}Th ($^{234}Th_{xs}$) is ^{234}Th that is not in secular equilibrium with the ^{238}U parent present in the uppermost sediments, presumably because it was supplied by settling particles. Supported ^{234}Th, in equilibrium with ^{238}U present in the sediment, is identified at the core depth below which no further decrease in ^{234}Th activities is observed ("Equilibrium Depth"; EQ). The supported activity is subtracted from the total activity to derive $^{234}Th_{xs,0}$ (Eq. 6).

$$^{234}Th_{xs,0} = \left(Decay\ Corrected\ ^{234}Th\right) - Supported\ ^{234}Th\ (dpm\ g^{-1}) \quad (6)$$

Sediment inventories of $^{234}Th_{xs,0}$ were multiplied by dry bulk density (~ 0.1 g cm^{-3}), and decay constant of ^{234}Th (0.0288 d^{-1}) and integrated from 0 to the EQ (~ 2 – 4.5 cm) to derive the sediment accumulation flux of $^{234}Th_{xs}$ on the sea floor (Eq. 7).

$$Sediment\ Accumulation\ Flux\quad {}_{^{234}Th} = \int_0^{EQ} \lambda Th\ (^{234}Th - {}^{238}U)\ dz = \int_0^{EQ} \lambda(^{234}Th_{xs,0})dz \quad (7)$$

Finally, to derive the sediment accumulation flux of POC, following Eq. 4, the ^{234}Th sediment accumulation flux (Eq. 7) are multiplied with the water column (a) large and (b) small particle POC:^{234}Th ratios measured at 65 m, the depth which represents particles that are about to settle on the seafloor (70 m). Organic carbon content in sediments was measured on an Elemental Analyzer (Elementar MicroCube & Isoprime 100) at Dalhousie University. The POC:^{234}Th ratios directly measured in the sediment are not used as ^{234}Th decays away faster than OC is respired in sediments.

3. Results

https://doi.org/10.5194/egusphere-2025-2493
Preprint. Discussion started: 17 June 2025

3.1 Hydrography of Bedford Basin in 2021 – 2024

Hydrographic conditions in the Bedford Basin (2021 – 2024) generally align with long term trends (Li & Harrison, 2008; Haas et al., 2021). Winter and spring surface cooling reduce summer stratification and drive vertical convection (Fig. 2a). However, 2021 saw higher sea surface temperatures (SSTs), leading to stronger stratification (Rakshit et al., 2023), and a lack of shelf water intrusions (Fig. 2e). That year, bottom waters experienced a six-week oxygen minimum, in contrast with records from 2014 – 2020 when mixing and intrusions increased dissolved oxygen in the Bedford Basin (Haas et al., 2021). The absence of winter mixing in 2021 may be linked to warmer air temperatures from January – March 2021 (- 0.2 °C), compared to the long-term mean (Government of Canada, 2018) at this site (- 1.5 °C). A spring phytoplankton bloom followed the cessation of winter mixing (Fig. 2d), with chlorophyll maxima at 5 – 10 m depth. The 2021 bloom, as denoted by chlorophyll-a (chl-a) signals, was relatively weak, (11.1 mg m^{-3}) compared to stronger blooms observed in 2022 and 2023. The largest spring bloom sampled in this study occurred in 2023 (34.9 mg m^{-3} chl-a). Deep chl-a signals are observed down to 70 m depth in some sampling events (May 2023). A secondary fall bloom occasionally occurred, including one in late summer 2021 (15.4 mg m^{-3} chl-a). Two intrusion events were observed during throughout 2021 – 2024 (Nov 2022, Jan 2024; Fig. 2e).

https://doi.org/10.5194/egusphere-2025-2493
Preprint. Discussion started: 17 June 2025

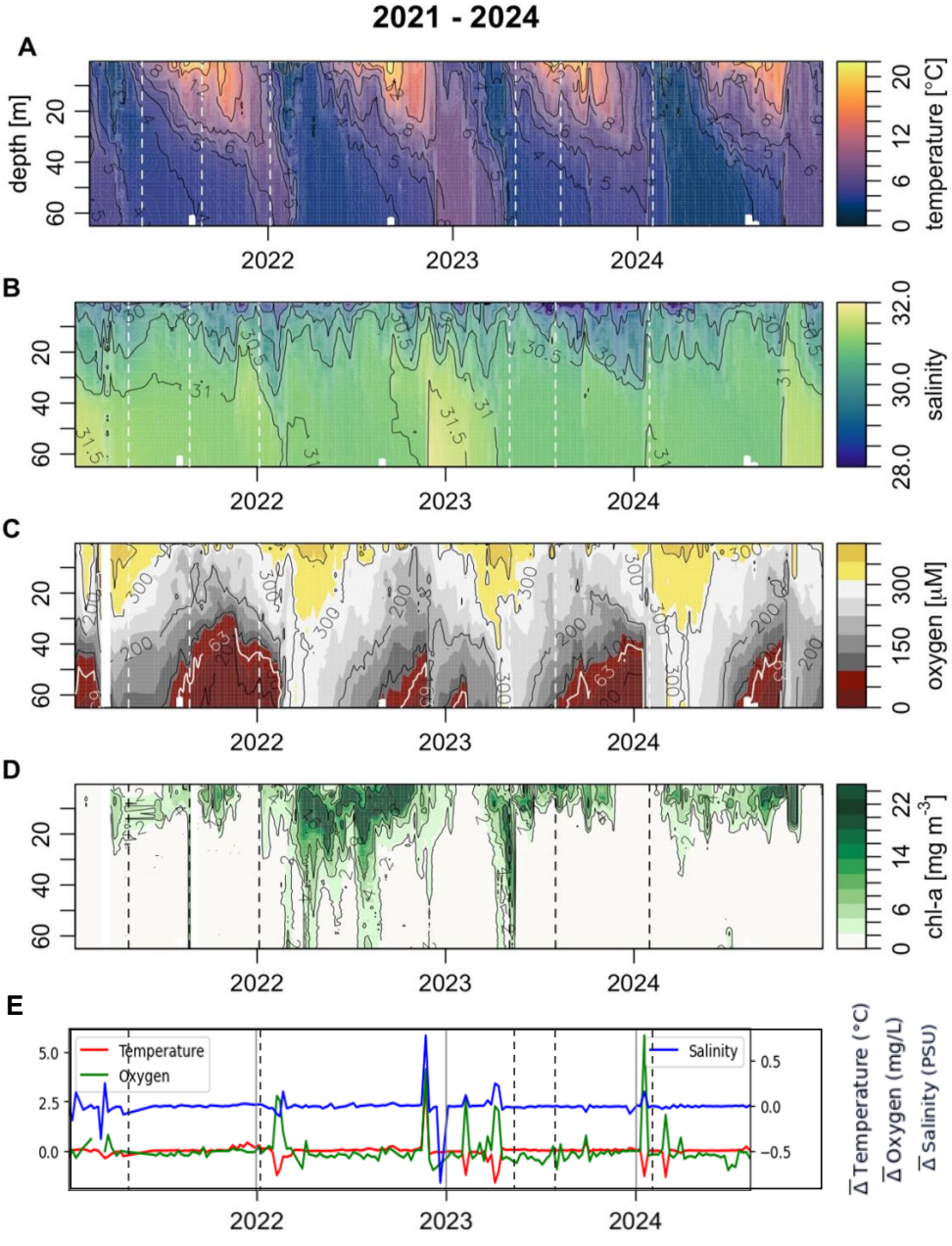

Figure 2. Hydrographic conditions in Bedford Basin (Compass Buoy Station) from 2021 – 2024. Time series of a) Temperature (°C), b) Salinity (PSU), c) Oxygen concentration (µM), d) Chl-a concentration (mg m^{-3}), e) Anomalies of temperature, oxygen concentration and salinity, which trace the intrusion of shelf waters into the basin. A zero anomaly represents no variation between T,S,O between weeks. Dashed lines in all panels represent the sampling events in this study.

https://doi.org/10.5194/egusphere-2025-2493
Preprint. Discussion started: 17 June 2025

3.2 Total ^{234}Th in the water column

Throughout the water column, $^{234}Th_{tot}$ activities displayed large deficits ($^{234}Th_{tot}$ = 0.1 – 1.1 dpm L^{-1}) compared to ^{238}U activities (mean = 2.09 ± 0.04 dpm L^{-1}) at all sampling events and all depths (Fig. 3). This indicates that the particle flux in Bedford Basin was large enough in the entire water column to scavenge ^{234}Th prior to its decay. Similar observations have been made in the few other studies from coastal regions (e.g., Luo et al., 2014; Wei and Murray, 1992, Black et al., 2023, Lepore et al., 2007). This contrasts with open ocean sites where ^{234}Th deficits are typically restricted to the euphotic zone (Owens et al., 2014). Generally, in each season, consistency is seen between years, with some variation that could be due to differences in bloom timing, productivity, etc. The largest deficit, with ^{234}Th activities as low as 0.1 dpm L^{-1}, occurred during the large bloom event in May 2023 (Fig. 3d), suggesting enhanced scavenging during this time. Winter profiles (Fig. 3c) are more uniform with depth compared to spring and summer, and despite low productivity during these times (Fig. 2d), still show a pronounced deficit throughout the entire water column.

3.3 Size fractionated particulate ^{234}Th and POC activities in water column

Along with $^{234}Th_{tot}$, size fractionated particulate ^{234}Th ($^{234}Th_p$) were obtained at approximately 20, 40, 60 m depths by in-situ pumps. At all depths, the small (1 – 51 µm) particle fraction dominated the $^{234}Th_p$ activities (93%) and POC concentration (77.4%), suggesting a large amount of POC is suspended on particles in the water column (Fig. 4). Mean $^{234}Th_p$ activities on large size fraction particles were 0.06 ± 0.04 dpm L^{-1} (Fig. 4) and were highest during bloom events. This value is significantly larger than first measurements of $^{234}Th_p$ in the Bedford Basin (0.008 ± 0.006 dpm L^{-1}, Black et al., 2023), likely due to a difference in methods (see Section 4.4). Mean $^{234}Th_p$ activities on the small size fraction (0.8 ± 0.3 dpm L^{-1}) were higher than those on large particles. Although dissolved ^{234}Th ($^{234}Th_{diss}$) was not measured in this study, subtracting $^{234}Th_p$ from the $^{234}Th_{tot}$ at the same approximate depth provides an estimation. The activity of dissolved ^{234}Th in Bedford Basin is consistently low and nearly devoid (0 – 0.6 dpm L^{-1}), a finding that is similar in other coastal fjords (e.g. Luo et al., 2014). Hence, the majority of $^{234}Th_{tot}$ is in the $^{234}Th_p$ pool, consistent with other studies in the Bedford Basin (Black et al., 2023; Niven et al., 1995). Particulate organic carbon (POC) on the large particle fraction (Fig. 4) had a mean of 1.0 ± 1.2 µM, while POC on the small particle fraction had a mean of 4.5 ± 3.1 µM. The residual activity of particulate ^{234}Th (Ra_{P234}) reveal that residual beta counts were higher than the detection limit in 38% of the small particulate samples, but no counts exceeding the detection limit were found on the large particles.

https://doi.org/10.5194/egusphere-2025-2493
Preprint. Discussion started: 17 June 2025

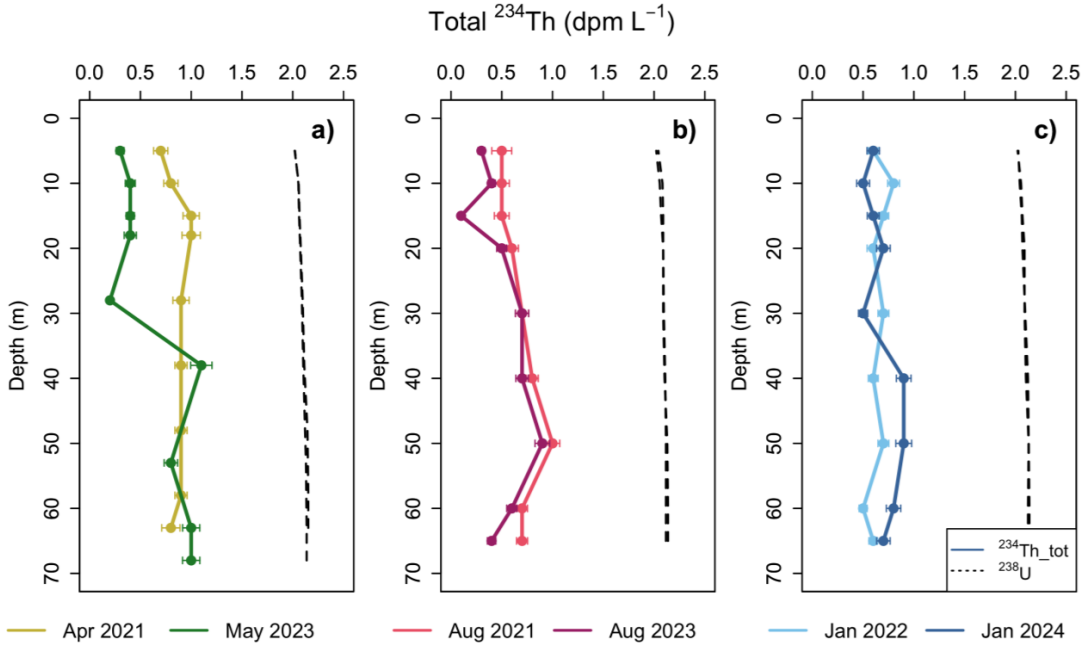

Figure 3. Water column profiles of total ^{234}Th (dpm L^{-1}) activity in each season sampled. a) Spring (April, May), b) Summer (August), c) – Winter (January) compared to ^{238}U activity (dpm L^{-1}) derived from salinity (Owens et al., 2011).

https://doi.org/10.5194/egusphere-2025-2493
Preprint. Discussion started: 17 June 2025

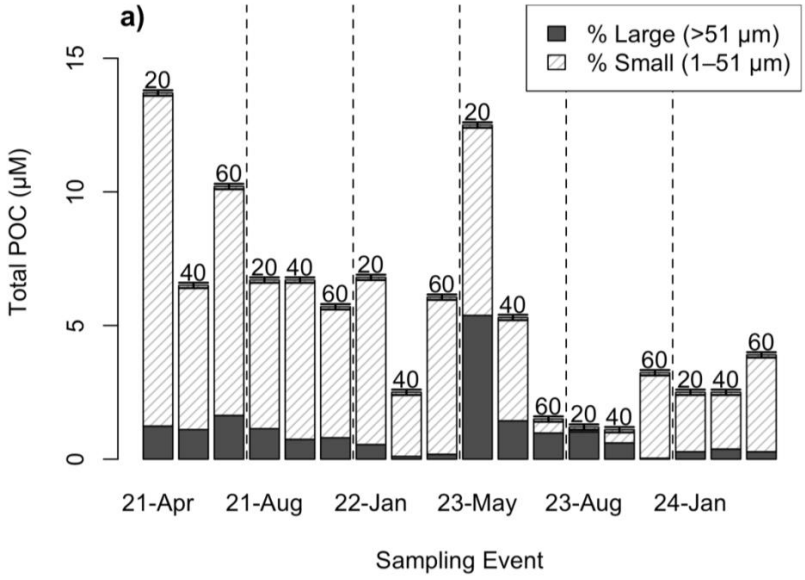

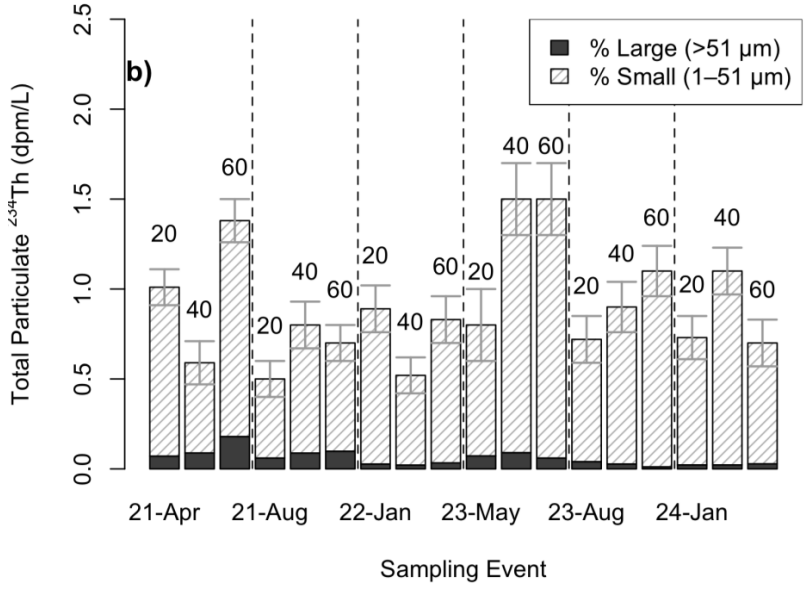

390

Figure 4. Size fractionated measurements of a) total particulate organic carbon (µM) and b) total particulate ^{234}Th (dpm L^{-1}) at each water depth (~ 20, 40, and 60 m) on each sampling event. Total particulate ^{234}Th is equal to the sum of the large (> 51 µM) and small (1 – 51 µM) particles. The small particle fraction is consistently associated with higher particulate ^{234}Th and POC and ^{234}Th concentrations. Dashed lines separate sampling events.

395

https://doi.org/10.5194/egusphere-2025-2493
Preprint. Discussion started: 17 June 2025

Table 1. Water column ^{234}Th cumulative fluxes measured at the bottom of the Bedford Basin (60 – 65 m). POC:^{234}Th ratios measured on large and small particles measured at 60 – 65 m (large volume pumps) and POC fluxes derived by multiplying ^{234}Th cumulative fluxes by large and small POC:^{234}Th ratios, calculated from a steady-state Th model. Asterisk (*) represents data from Black et al. (2023) with data from a pilot study in 2019.

Sampling Event	Sampling Date (M-D-Y)	Season	Water column ^{234}Th flux dpm m^{-2} d^{-1}; 60 – 65 m)	Large particle POC:^{234}Th; µmol C/dpm^{-1} 60 - 65m)	LSF POC flux (mmol m^{-2} d^{-1}; 60 – 65 m)	Small particle POC:^{234}Th; 60 – 65 m)	SSF POC flux mmol m^{-2} d^{-1};60 – 65 m)
April 2019*	4-11-2019	Spring	2140 ± 160	340 ± 10	780 ± 190	11 ± 4	25 ± 1020
May 2019*	5-09-2019	Spring	1890 ± 150	920 ± 4	2070 ± 500	11 ± 6	20 ± 10
April 2021	04-27-2021	Spring	2205 ± 64	9.1 ± 1	20.1 ± 2.3	7.1 ± 1	15.1 ± 1.2
May 2023	05-05-2023	Spring	2767 ± 62	67 ± 8.3	44.5 ± 4.1	0.3 ± 0.07	0.8 ± 0.2
August 2019*	08-02-2019	Summer	2020 ± 150	500 ± 300	710 ± 170	60 ± 20	150 ± 40
August 2021	08-23-2021	Summer	2537 ± 61	8.1 ± 1	20.5 ± 2.1	7.7 ± 1	19.6 ± 3.0
August 2023	08-02-2023	Summer	2726 ± 50	1.3 ± 0.6	3.6 ± 1.7	2.9 ± 0.4	8.0 ± 0.6
January 2022	01-05-2022	Winter	2603 ± 46	4.1 ± 0.6	10.6 ± 1.5	7.3 ± 1.2	19.0 ± 3.1
January 2024	01-31-2024	Winter	2478 ± 54	8.3 ± 0.7	20.8 ± 1.5	4.9 ± 0.9	12.2 ± 2.1

https://doi.org/10.5194/egusphere-2025-2493
Preprint. Discussion started: 17 June 2025

3.4 POC:^{234}Th ratios on large and small particles

In general, POC:^{234}Th on both the large and small particle fractions are < 20 µmol C/dpm^{-1} (Fig. 5) and were variable. On average, higher POC:^{234}Th ratios on the larger particles were observed compared to the smaller particles ($p < 0.01$), consistent with open ocean studies (Charette and Moran, 1999). This trend was most driven by two distinct high ratios on the large fraction in the 0 – 20 m depth range (May 2023, August 2023), likely driven by a strong chl-a signal at these times (Fig. 2d). The POC:^{234}Th ratio on the large and small fraction had a mean of 16.2 ± 14.3 (range 1.3 – 67) and 5.8 ± 4.1 (0.2 – 13.2) µmol C/dpm^{-1} respectively. The POC:^{234}Th ratio generally decreased with depth on the large fraction, but not on the small fraction which showed no pattern with depth (Fig. 5). On average, the large fraction POC:^{234}Th ratios are a factor of ~ 2.8 x larger than the small POC:^{234}Th ratios.

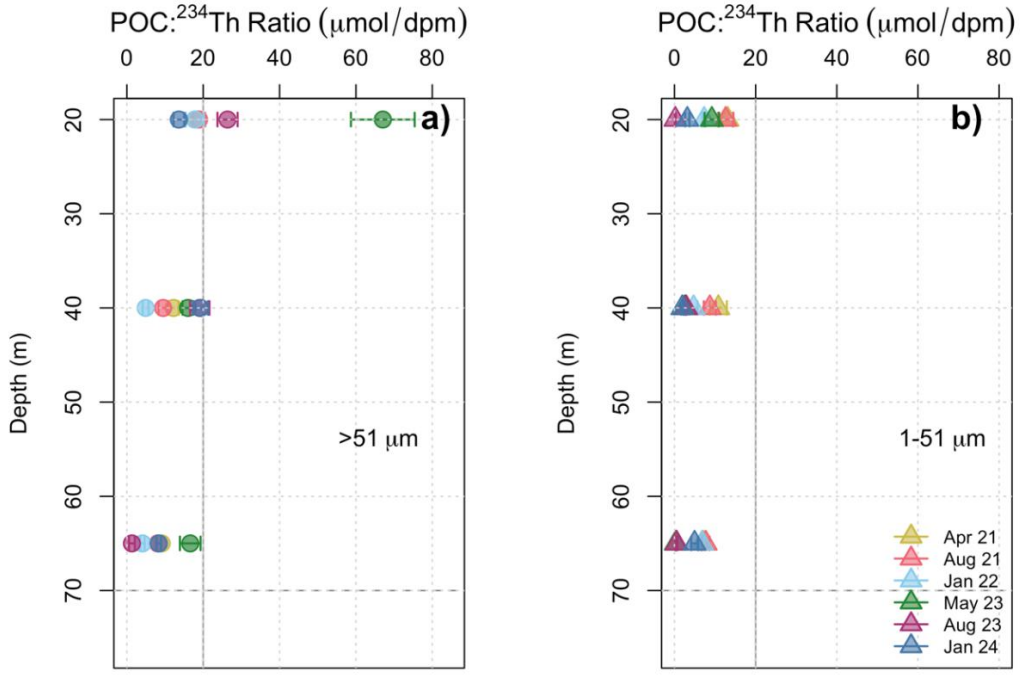

Figure 5: Water column ratios of particulate organic carbon to ^{234}Th (POC:^{234}Th, µmol C/dpm^{-1}) in each sampling event throughout 2021 – 2024. Error bars indicate propagated uncertainties associated with measurements. a) POC:^{234}Th on the large size fraction particles (> 51 µM). b) POC:^{234}Th on the small size fraction particles (1 – 51 µM). Other than a few large POC:^{234}Th ratios that correspond with greater chl-a in the water column, the POC:^{234}Th ratios are similar in magnitude on both size fractions (< 20 µmol C/dpm^{-1}, grey reference line). The dashed grey line at 70 m represents the bottom of the Bedford Basin.

3.5 Water column fluxes of ^{234}Th and POC

3.5.1 ^{234}Th fluxes

https://doi.org/10.5194/egusphere-2025-2493
Preprint. Discussion started: 17 June 2025

Cumulative ^{234}Th fluxes increase nearly linearly with water depth (R^2 = 0.95) and do not show much seasonal variation (Fig. 6a). Interestingly, similar observations were made in other coastal sites such as Dabob Bay, Washington (Wei and Murray, 1992), Saanich Inlet, British Columbia (Luo et al., 2014), Beaufort Sea Shelf (Baskaran et al., 2003), and Mecklenburg Bay, Baltic Sea (Forster et al., 2009). Combining the data from the linear regression of all dates reveals a water column rate increase with depth of 37 dpm m^{-2} d^{-1}, larger than previously measured in spring summer 2019 (31 dpm m^{-2} d^{-1} ; Black et al., 2023). The mean (± s.d.) water column ^{234}Th fluxes at ~ 65 m and interpolated to 70 m were 2638 ± 238 and 2842 ± 224 dpm m^{-2} d^{-1} respectively.

3.5.2 POC fluxes derived with the large and small particle size fraction

POC export fluxes (Fig. 6) were calculated following Eq. 4 and using the >51 µm POC:^{234}Th ratio (Fig. 5a). POC fluxes at the deepest depth sampled (60 – 65 m) had a mean (± s.d.) of 20 ± 14 mmol C m^{-2} d^{-1} (Fig. 7A) and ranged from 3.6 ± 1.1 to 44.5 ± 4.1 mmol C m^{-2} d^{-1}. Highest POC flux values were seen in May when chl-a was at its highest (Fig. 6b), and in general, POC fluxes derived with the large size fraction followed a high-low pattern with depth (Martin et al., 1986). Modest POC fluxes were still prevalent in boreal winter estimates, averaging 15.7 ± 7.2 mmol C m^{-2} d^{-1}. One of these winter sampling events occurred around the time of an intrusion event in the BB, and it is possible that this event brought it additional POC from nearby shelf waters (see Section 4.2). Disregarding this sampling event, POC fluxes in January 2022 were 10.6 ± 1.5 mmol C m^{-2} d^{-1}. Comparing to the other size fraction analyzed in this study, POC export fluxes were also calculated following Eq. 4 and using the 1 – 51 µm POC:^{234}Th ratio (Fig. 5b). These small particle fluxes at 65 m had a mean (± s.d.) of 12.5 ± 7.1 (Fig. 7b) and ranged from 0.8 to 19.6 mmol C m^{-2} d^{-1}. No clear pattern with depth was observed in the small particle fluxes (Fig. 6c).

https://doi.org/10.5194/egusphere-2025-2493
Preprint. Discussion started: 17 June 2025

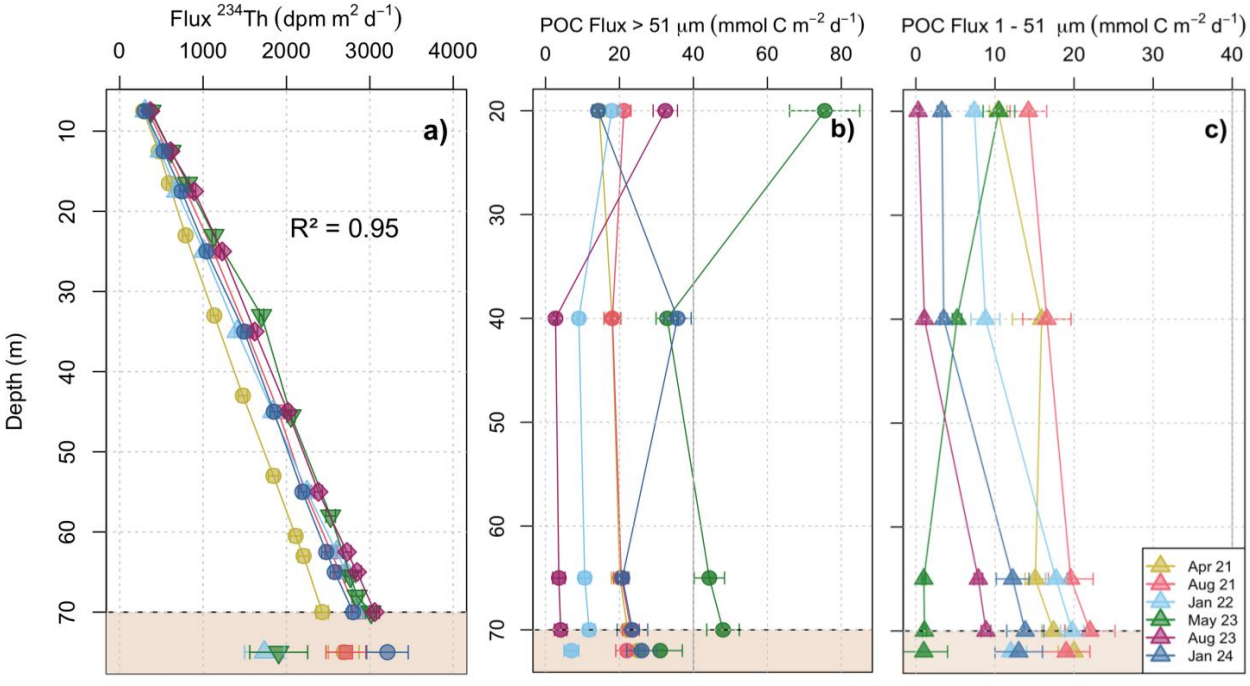

Figure 6: a) Bedford Basin 1D steady state fluxes in 2021 – 2024. Profiles of Cumulative ^{234}Th flux in the water column compared to decay corrected excess ^{234}Th ($^{234}Th_{xs,0}$) in the topmost sediment. Sediment inventories of $^{234}Th_{xs}$ were integrated from ~ 0 – EQ depth (~ 2 – 4.5 cm) to derive accumulation of $^{234}Th_{xs}$ on the sea floor. The resulting sediment fluxes (i.e. sediment accumulation flux) are shown below the approximate depth of the sediment-water interface (dashed line). POC fluxes were derived at a given depth with the steady state model with estimates obtained from Eq. 4 on the b) large particle POC:^{234}Th ratio and c) small particle POC:^{234}Th ratio. The sediment accumulation flux was also multiplied by the water column POC:^{234}Th ratios (at 60 – 65 m) to derive POC sediment accumulation flux. Note the change in scale between the plots and the grey reference line at 40 mmol C m^{-2} d^{-1}. No sediment core was taken in August 2023.

https://doi.org/10.5194/egusphere-2025-2493
Preprint. Discussion started: 17 June 2025

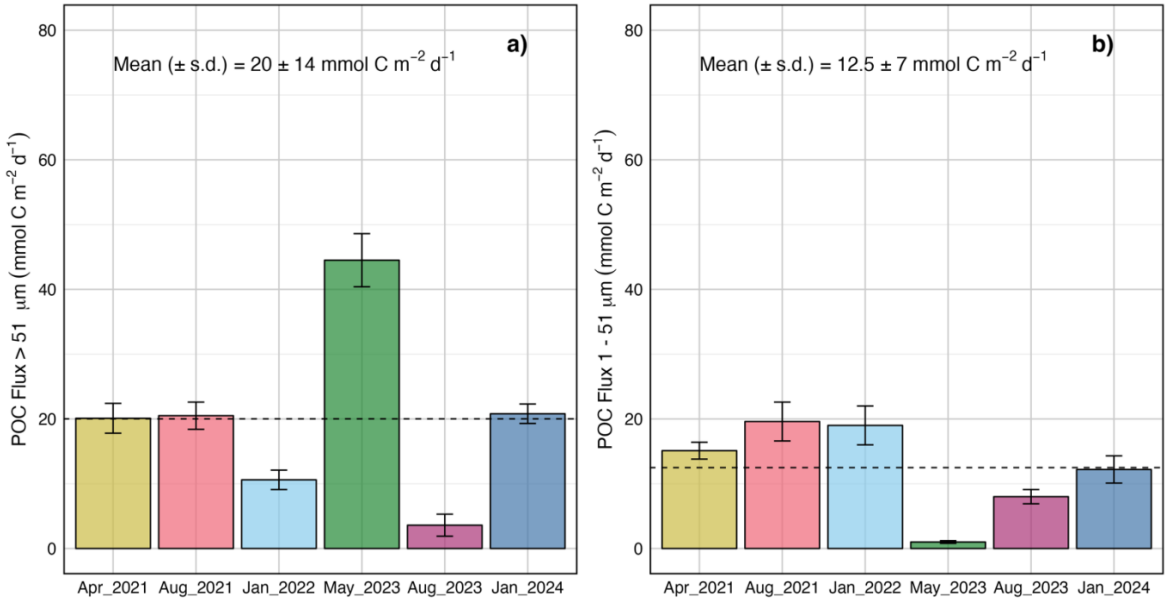

Figure 7: Measured ^{234}Th-derived mean (± s.d.) particulate organic carbon fluxes deposited to the near bottom (~ 65 m) of the Bedford Basin on the a) large particle (> 51 µm), and b) small particle (1 – 51 µm) size fractions. The dashed black line represents the mean POC flux for each size fraction respectively.

3.6 Sediment accumulation fluxes of ^{234}Th and POC

The equilibrium depth was always observed by ~ 4.5 cm core depth, with the majority of excess ^{234}Th ($^{234}Th_{xs,0}$) confined to the top ~ 2 – 4.5 cm of every core. Excess ^{234}Th in the EQ was variable in each sampling event, averaging 15.3 ± 16 dpm g^{-1} and ranging from 4.8 – 46 dpm g^{-1} (Fig. 8a). Generally, the activity of $^{234}Th_{xs0}$ rapidly decreased downcore, likely due to decay of ^{234}Th after deposition in the seabed. The mean supported ^{234}Th (from 4.5 – 6 cm) was 2 ± 0.5 dpm g^{-1}. The mean sedimentary POC concentrations and percentage of POC in sediments was 4.9 ± 0.4 mmol C g^{-1} and 5.7% ± 0.3 respectively and were consistent with core depth between 0 – 4 cm. The POC:^{234}Th ratios in sediments are an order of magnitude larger than those in water column, ranging from 103 – 3257 µmol dpm^{-1} (Fig. 8b). This likely reflects the more rapid decay of ^{234}Th relative to the remineralization of organic carbon on the seabed. These ratios increased with core depth, corresponding with deceasing $^{234}Th_{xs,0}$ activity (Fig. 8b). The sediment accumulation fluxes of ^{234}Th flux had a mean (± s.d.) of 2450 ± 549 dpm m^{-2} d^{-1} and ranged from 1735 ± 237 to 3211 ± 249 dpm m^{-2} d^{-1} (Table 2). The ^{234}Th sediment accumulation fluxes were multiplied by the POC:^{234}Th ratio of water column particles collected at the bottom of the basin (60 – 65 m) to derive POC sediment accumulation fluxes. The mean (± s.d.) POC sediment accumulation flux derived with the large particle fraction was 22 ± 9 mmol C m^{-2} d^{-1}, larger than the mean POC flux derived with the small particle fraction of 13 ± 8 mmol C m^{-2} d^{-1} (Fig 6b, Fig 6c).

https://doi.org/10.5194/egusphere-2025-2493
Preprint. Discussion started: 17 June 2025

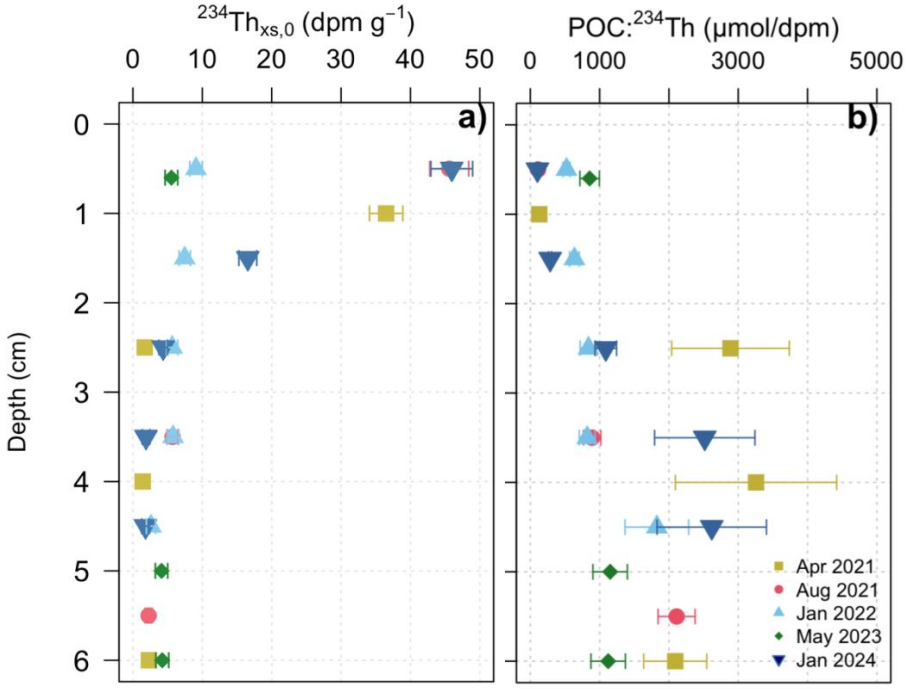

Figure 8: a) Sediment downcore profile of decay corrected excess ^{234}Th, derived from subtracting the supported ^{234}Th from decay corrected ^{234}Th in sediments. The supported ^{234}Th is identified at the core depth below which no further decrease in ^{234}Th activities is observed. b) the ratio of POC:$^{234}Th_{xs,0}$ in sediments.

Table 2. Bedford Basin sediment accumulation fluxes of ^{234}Th (dpm m^{-2} d^{-1}) in each sampling event in 2021 – 2024. This is calculated by multiplying the integrated activities of $^{234}Th_{xs,0}$ (0 – EQ depth) by the dry bulk density (0.1 g cm^{-3}) and decay constant for ^{234Th} (0.0288 d^{-1}).

Sampling Event	Sampling Date (M-D-Y)	Season	^{234}Th sediment accumulation flux (dpm m^{-2} d^{-1})
April 2021	04-27-2021	Spring	2687 ± 184
May 2023	05-05-2023	Spring	1907 ± 347
August 2021	08-23-2021	Summer	2713 ± 239
January 2022	01-05-2022	Winter	1735 ± 237
January 2024	01-31-2024	Winter	3211 ± 249

https://doi.org/10.5194/egusphere-2025-2493
Preprint. Discussion started: 17 June 2025

4 Discussion

4.1 A general match between water column ^{234}Th flux and surficial sediment ^{234}Th accumulation flux

This study demonstrates the utility of coupled water column-sediment ^{234}Th measurements in assessing coastal carbon fluxes using a 1D steady-state model. To the best of our knowledge, few studies have applied a coupled water column-sediment approach to explore the ^{234}Th/^{238}U method in support of coastal carbon budget quantifications (Cochran et al., 1976; Charette et al., 2001, Lepore et al., 2007). The present study, along with the first coupled measurements in Bedford Basin made in 2019 (Black et al., 2023), demonstrates a close match between the flux at the bottom of the water column and the uppermost sediments beneath it. Overall, the mean (± s.d.) 2021 – 2024 sediment accumulation of ^{234}Th of 2261 ± 512 matches within error to the mean water column flux (interpolated to 70 m) of 2851 ± 249 (Fig. 6a). A paired t-test revealed no statistically significant difference between the water column and sediment fluxes, with a mean difference (± s.d.) of 349 ± 747 dpm m^{-2} d^{-1} (t = 1.04; df= *4,* p=0.30). When data from 2019 (Black et al., 2023) are included, the mean difference (± s.d.) is even smaller (184.1 ± 836) and not statistically significant (t = 0.6; df=*7,* p=0.5), suggesting that the observed difference may be due to random variability. The mean ratio between water column and sediment ^{234}Th fluxes is 1.1 indicating close agreement between the two, with the water column flux being slightly higher than the sediment flux. This finding implies that on the timescales of weeks to ~ 100 days, no major particle loss is occurring, and particles are generally not being exported out of the basin. A similar finding was first made by Cochran et al. 1995, who found a water column-sediment inventory match within a factor of 2 in both 1992 and 1993 on the Northeast Water Polynya off Greenland. Likewise, in their comparison of model predicted ^{234}Th water column inventory vs sediment inventories in the upper 0 – 5 cm of the Gulf of Maine, Charette et al. (2001) find that inventories were within a factor of 2 of the predicted values, with a ratio of 1.1. These findings suggest that Bedford Basin is a promising location for more complex observational studies of particle dynamics, and opens the opportunity to study other short-lived radioisotopes, such as Bismuth-210 (^{210}Bi; $t_{1/2}$ = 5 d) to study particle dynamics on a finer temporal resolution (hours to days; see Yang et al., 2022).

4.2 A persistent year-round deficit of ^{234}Th in the water column

A notable feature of this study is the persistent deficit of ^{234}Th relative to ^{238}U in all seasons sampled. Similar has been found in other shallow basins (Luo et al., 2014; Charette et al., 2001; Evangeliou et al., 2011, Amiel & Cochran., 2007). This persistent deficit suggests that i) particle scavenging of ^{234}Th is occurring throughout the entirety of the water column (0 – 70 m) and ii) the scavenging rate is high enough to continually maintain a lower ^{234}Th activity relative to ^{238}U. Scavenged particles in the Bedford Basin may originate from both biological processes in the upper 30 m (Fig. 3), and resuspended particles. Resuspension from the seafloor could be a source of particles to deep waters, however we find that the sedimentary POC:^{234}Th ratio is an order of magnitude higher than those in the water column (Fig 8b), likely due to the temporal decay of ^{234}Th exceeding the remineralization of POC. Bottom resuspension would be expected to introduce particles with these elevated POC:^{234}Th which is not reflected in deep water column POC:^{234}Th ratios from this study. Lampitt (1985) proposed that resuspension only occurs if the sediment-water interface is composed of a detrital layer. In the Bedford Basin, evidence of a nepheloid layer, rather than a detrital layer at the sediment-water interface has been reported (Azetsu-Scott and Johnson, 1994, Black et al., 2023), providing evidence against major resuspension from bottom sediments. However, given the concave bathymetric profile of the Bedford Basin (Fig. 1), resuspended sediments could be "funneled" into the Compass Station from the sides (Trimble & Baskaran, 2005). In this study, we observe a strong signal of resuspension at mid depths in April 2021, as well as a weaker signal of resuspension at 60 m in the summer and winter sampling events (Fig. 9), though only on the small particle fraction. This Ra_{p234} signal provides

https://doi.org/10.5194/egusphere-2025-2493
Preprint. Discussion started: 17 June 2025

indication that some lateral resuspension of fine particles is likely occurring in the basin and is reason to report POC fluxes using the large particle fraction. Furthermore, deep and extensive CTD-derived chl-a fluorescence signals (Fig. 2d) suggest that biological processes could also be responsible for particle creation and continued scavenging in deeper waters. These features are not unique (Black et al., 2023), and fluorescing material has been found at depths > 3000 m in the Arctic as a result of a rapid bloom-collapse cycle (Boeitus et al., 2013). While additional data (e.g. UVP, net primary production (NPP), backscatter, etc.) are needed to identify the source for the evident fluorescence signals at depths much deeper than expected given the high particle load in the water column, these features could be the key to understanding the persistent Th deficits in the Bedford Basin.

The persistent deficit is also strong in boreal winter periods, when production is presumed to be at its lowest. Hargrave and Taguchi (1978) argued that inflows of dense surface water from intrusions could be rich in labile particulate organic matter (POM) and could deliver additional POC that could drive the moderate POC fluxes we see at this time. Therefore, the POC flux in January 2024 could be attributed to the intrusion event occurring around the same time. However, our sampling in January 2022 still yields a modest flux value of 10.6 ± 1.5 mmol C m^{-2} d^{-1} at 65 m. This is comparable to January 2024 (Fig. 7) but took place after a period of water column stability (Fig. 2e). A notable feature of this 2022 winter event is that POC fluxes are higher when using the small fraction to compute flux, yielding 17.7 ± 1.3 mmol C m^{-2} d^{-1} (Fig. 7b). Bolanos et al. (2020) recently proposed that smaller phytoplankton species (< 20 µm) are important members of the phytoplankton community in the North Atlantic. Robicheau et al. (2022) have shown that specific phytoplankton types have higher abundance values, especially in the early winter in the Bedford Basin when there are temperature anomalies. *Synechococcus* (of clades I and IV) have previously been identified as important in the Northwest Atlantic and were especially dominant in the subpolar region during winter months. Primary production was not measured in this study, but modelling efforts have shown that the NPP in the Bedford Basin is in the 100's of mmol C m^{-2} d^{-1} at peak times, and 10's of mmol C m^{-2} d^{-1} otherwise (Black et al., 2023), suggesting that lower NPP in winter months can still yield modest POC fluxes. This was also observed in the nearby Gulf of Maine (Charette et al., 2001) where POC fluxes of 14 ± 0.8 mmol C m^{-2} d^{-1} we're measured in the lower range of their NPP measurements (26.4 mmol C m^{-2} d^{-1}). These small cells could possibly be the driver of this distinct winter flux (most prominent in the small particle fraction) that we see in Jan 2022, though the reasoning behind the winter flux remains ambiguous. These results highlight the dynamic particle processes in Bedford Basin that maintain persistent ^{234}Th deficits, emphasizing the need for continued year-round, high-resolution particle and radionuclide measurements.

https://doi.org/10.5194/egusphere-2025-2493
Preprint. Discussion started: 17 June 2025

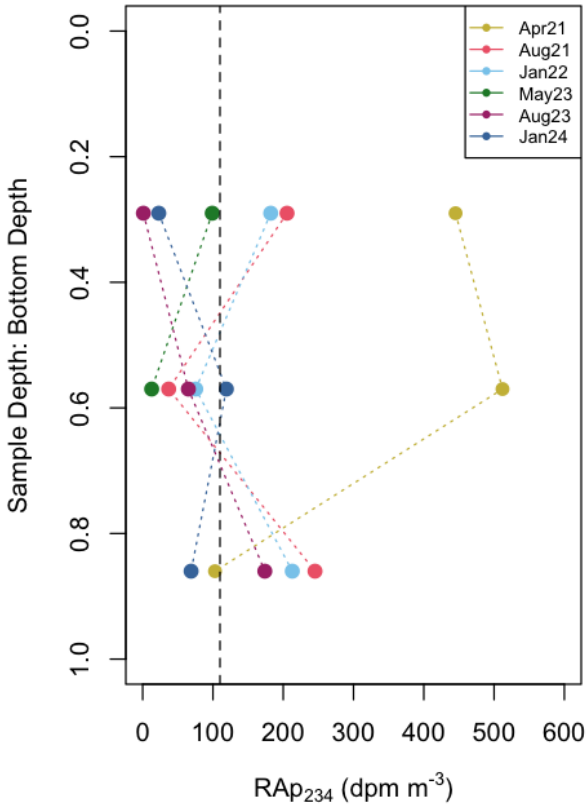

Figure 9: Total residual activity of particulate ^{234}Th (RA_{P234}) at the Compass Station. RA_{P234} values representing the sum of residual counts from both size fractions. The dashed vertical line is the detection limit (derived from filter blank analyses). Only RA_{P234} signals above the detection limit were found on the small particulate fraction.

4.3 Non-Steady State (NSS) Considerations

Steady-state (SS) dynamics are often assumed in coastal and open ocean ^{234}Th/^{238}U disequilibrium studies (e.g. Coale and Bruland, 1985, Foster and Shimmield, 2002) due to sampling constraints. The SS model is also applied here, as the successive measurements days-weeks apart, which are required for a NSS model, are not available. We explore the implications of NSS factors in this section. We assume that $\partial^{234}Th/\partial t$ is equal to 0 and the system is in steady state. The SS model assumes that i) ^{234}Th activities and removal rates are near constant with respect to ^{234}Th decay, ii) the contributions of vertical and horizontal advection of ^{234}Th are minor, and iii) scavenging is irreversible. Physical studies of the Bedford Basin have generally shown that 1D assumptions hold for most of the year (Burt et al., 2013). The circulation pattern of Halifax Harbour is characterized as a two-layer, estuarine-type system, with a fresher upper layer flowing seaward, driven by inflows from the Sackville River, and a saltier deep-water return flow (Fader and Miller, 2008). However, with a mean surface outflow of 0.2 cm s^{-1}, this circulation is weakest in the Bedford Basin (Burt et al., 2013). Despite an inflow from the open Atlantic, the presence of a sill largely prevents mixing below 20 m in the basin (Shan et al., 2011). Periodic deep vertical mixing, such as during an intrusion event could increase the potential to disrupt condition of the SS model. No major lines of evidence in the ^{234}Th activities are indicated in our study (no major RA_{P234} signals, or significant difference in POC:^{234}Th), and despite the intrusion in Jan 2024, the ^{234}Th activities

https://doi.org/10.5194/egusphere-2025-2493
Preprint. Discussion started: 17 June 2025

are similar between Jan 2024 (intrusion) and Jan 2022 (no intrusion). NSS impacts (i.e., rapid temporal changes in ^{234}Th activities) have been shown to play a role on flux calculations during a phytoplankton bloom (Buesseler et al., 1992). Black et al. (2023) estimated a maximum contribution of + 70 ± 140 dpm m^{-2} d^{-1} during a bloom transition period in the Bedford Basin. Given the mean water column export in this study of 2638 ± 238 dpm m^{-2} d^{-1}, this max NSS contribution is < 3 %. If feasible, future studies in the basin should sample on a finer temporal resolution (1 – 4 weeks) to better understand NSS contributions in the basin.

4.4 Revisiting ^{234}Th activities on > 51 µm particles

A key source of uncertainty in estimating POC fluxes using ^{234}Th/^{238}U disequilibrium is the POC:^{234}Th ratio used for filtered particles, which has led to inconsistent flux estimates in previous studies (Lalande et al., 2008). Determining the most representative POC:^{234}Th ratio remains an active area of research (e.g. Buesseler et al., 2006; Puigcorbe et al., 2020) to ensure accurate flux measurements. In the Bedford Basin, we find the primary source of variability in POC flux estimates is the POC:^{234}Th ratio of large (>51 µm) particles. Previously, Black et al. (2023) reported ratios in the Bedford Basin > 900 µmol dpm $^{-1}$, yielding exceptionally large fluxes (~2100 mmol C m^{-2} d^{-1}, Table 1), over an order of magnitude greater than predicted coastal carbon export models (Siegel et al., 2014). By contrast, this present study finds lower, more modest fluxes (< 70 mmol C m^{-2} d^{-1}), consistent with other coastal studies (< 200 mmol C m^{-2} d^{-1}, Luo et al., 2014; Cai et al., 2015; Cochran et al., 1995). High POC:^{234}Th ratios (> 100 µmol dpm $^{-1}$) have been previously linked to seasonal variability (Charette et al., 2001), however, the extreme values in Black et al. (2023) likely result from the differences in particle collection & delayed counting of beta emissions. Variations in sampling approaches highlight the potential for significant differences in POC measurements. Black et al. (2023) used a vacuum filtration system on Niskin-bottle collected samples, while this study employed McLane ™ Large Volume Pumps that filter in-situ. In their comparative study (Graff et al., 2023) found that in-situ pump sampling resulted in substantially lower POC compared to Niskin sampling at similar depths. This difference may arise due to variability in filtration speed, particle solubilization (Buesseler et al., 1995), and size fractionation (Hung et al., 2012). The methodological differences suggest that the elevated large particle POC:^{234}Th ratios reported by Black et al. (2023) likely result from sampling artifacts rather than true variability in particle flux. The ratios obtained in this study provide a more representative measure of large particle POC:^{234}Th at this site. To improve comparability, future studies in the Bedford Basin and other coastal regions should adopt consistent sampling methods to minimize methodological biases.

4.5 POC export in the Bedford Basin and an estimated C budget

The POC export fluxes derived in this study are in good agreement with other biogeochemical measurements taken in the Bedford Basin (Table 3). The mean depositional organic carbon flux (at 65 m), derived here from the large particle POC:^{234}Th ratio and integrated ^{234}Th flux was 20 ± 14 mmol C m^{-2} d^{-1} (Fig. 7), two orders of magnitude lower than first estimates of ^{234}Th-dervied POC flux (Black et al., 2023). This is a similar range as the nearby Gulf of Maine (34 ± 44 mmol C m^{-2} d^{-1}; March, June, September; Charette et al., 2001), Saanich Inlet in western Canada (11.5 ± 4 mmol C m^{-2} d^{-1} ; Luo et al., 2014), Greenland continental shelf (25 ± 14 mmol C m^{-2} d^{-1}; Cochran et al., 1995), and Norwegian fjords (21.9 – 24.4 mmol C m^{-2} d^{-1}; Wassmann, 1984). Our measured values are also similar to model estimates of organic carbon deposition flux in the Bedford Basin (25.2 mmol C m^{-2} d^{-1}; Rakshit et al., 2025), and sediment trap estimates at 60 m (17 mmol C m^{-2} d^{-1}; Hargrave and Taguchi., 1976). Translated to an annual molar estimate, (assuming our spring, summer, winter mean is representative of the year, and multiplying the mean daily flux by 365), our study reveals that 7.2 ± 1 mol C m^{-2} yr^{-1} is delivered to the seafloor annually, similar to annual

https://doi.org/10.5194/egusphere-2025-2493
Preprint. Discussion started: 17 June 2025

mean trap estimates in the BB of 6.2 mol C m^{-2} yr^{-1} (Hargrave and Taguchi, 1976). The modeled daily benthic carbon flux in the BB of 19 mmol C m^{-2} d^{-1} (Black et al., 2023), is equivalent to an annual export of ~ 7 mol C m^{-2} yr^{-1}, also consistent with our ^{234}Th-based estimates.

Using the mean weight % POC in the upper 5 cm of the sediment cores (5.7%), mean sedimentation rate (0.2 cm yr^{-1}; Black et al., 2023) and mean dry bulk density (275 kg m^{-3}), we find an organic carbon burial rate of 6.9 mmol C m^{-2} d^{-1}. This burial rate, combined with our mean POC depositional flux at 65 m, implies that the carbon burial efficiency is ~ 33%, larger than previous estimates at this site (10%; Black et al., 2023), and similar to other coastal zones (Faust and Knies., 2019). The remaining ~ 67% of the depositional POC is remineralized before burial, a finding consistent with measured dissolved inorganic carbon (DIC) fluxes from the sediments (15.6 mmol DIC m^{-2} d^{-1}; Rakshit et al., 2025). These findings suggest that the Bedford Basin is an important site of organic carbon sequestration.

To better understand C dynamics in the ocean, carbon flux metrics have been developed that help define the efficiency of the Biological Carbon Pump in marine environments (Buesseler et al., 2020; Buesseler and Boyd 2009). The thorium export ratio (ThE-ratio) is the ratio of POC flux (based on ^{234}Th measurements) relative to NPP in the euphotic zone. To estimate the export efficiency in the Bedford Basin, we divide the annual mean primary production in the basin by the annual mean flux of POC measured in this study. Primary production is rarely measured directly in the Bedford Basin with only one record of NPP from incubation studies (50 mmol C m^{-2} d^{-1}; Platt, 1975). Black et al (2023) approximated an annual mean NPP of 66 mmol C m^{-1} d^{-1} using a model based on in-situ chl-a and PAR data. This NPP estimate is within the range of NPP estimates from the nearby Gulf of Maine (i.e., 26-399 mmol C m^{-2} d^{-1}; Charette et al., 2001). With this information, we can divide the mean POC export at the base of the euphotic zone (~20 m; 29.4 mmol C m^{-2} d^{-1}) by mean NPP and derive ThE ratios of 49%. This ThE ratio is comparable to other coastal sites (26%, Charette et al., 2001; 50%, Falkowski et al., 1988; 60%, Cochran et al., 1995). A ThE ratio of 49% suggests moderate export efficiency at our site. It is, however, important to note that our estimation relies on modeled NPP values, and updated in-situ measurements of NPP would yield a more precise value of these ThE estimates.

Table 3. An updated carbon budget of the Bedford Basin presented by fluxes of carbon in the Bedford Basin and the method used to derive them. [a]Cylindrical trap estimates (Hargrave and Taguchi, 1978); [b] (Rakshit et al., 2025), [c] (Black et al., 2023).

Carbon fluxes in the Bedford Basin		
a) Fluxes in the water column	**mmol C m^{-2} d^{-1}**	**Methodology**
Large particle POC flux (60-65 m)	20 ± 14	POC:^{234}Th
Small particle POC flux (60-65 m)	12 ± 7	POC:^{234}Th
Particulate flux (60 m)[a]	17	Cylindrical traps
Modelled POC flux[b]	25.2	Reaction-transport model
Modelled POC flux[c]	19	Chl-a
b) Fluxes in the sediment	**mmol C m^{-2} d^{-1}**	**Methodology**
Large particle sediment accumulation flux	22 ± 9	POC:^{234}Th

https://doi.org/10.5194/egusphere-2025-2493
Preprint. Discussion started: 17 June 2025

Small particle sediment accumulation flux	13 ± 8	POC:^{234}Th
Measured DIC flux[b]	15.6 ± 10.2	Pore-water extraction

5 Conclusions

This study demonstrates the utility of the coupled ^{234}Th water column–surficial sediment sampling approach by quantifying ^{234}Th and POC fluxes in the water column and surface sediments of Bedford Basin, a coastal fjord in the North Atlantic, over quasi-seasonal sampling campaigns from 2021 to 2024. Within the uncertainties of the ^{234}Th/^{238}U disequilibrium method and a steady state approach, we find that the integrated deficit of ^{234}Th in the water column matches the excess of ^{234}Th in the uppermost sediments well. The match suggests that, on a timescale of the ~ 100 days, the Bedford Basin is in balance with respect to ^{234}Th, and no major particle loss is occurring. There were significant deficits of ^{234}Th relative to its parent ^{238}U throughout the water column during all sampling events, including boreal winter. We conclude that the majority of $^{234}Th_{tot}$ in the Bedford Basin is associated with the particulate ^{234}Th pool, with a significant portion bound to the small (1 – 51 µm) particle fraction. Translated into POC fluxes, the observed deficits reveal a mean POC export flux to the seafloor of 20 ± 14 mmol C m^{-2} d^{-1}. This estimate is based on the integrated ^{234}Th flux between (0 – 65 m water depth) multiplied by the POC:^{234}Th ratio on large (>51 µm) particles and is on par with other carbon flux proxies in the area. Water column POC flux estimates showed no apparent trend with season, other than a slightly elevated flux corresponding to elevated chl-a in May 2023. Measurements of POC export in boreal winter reveal modest flux, despite lower chl-a signals at this time. We estimate a thorium export ratio of 49% and an organic carbon burial efficiency of 33%, higher than previously estimated at this site. Based on this data, we suggest that the biological carbon pump is moderately efficient in the Bedford Basin, and that this site, like many other coastal areas, is an important site of organic carbon sequestration.

Data Availability

Data available upon request. Data will be uploaded to https://www.bco-dmo.org/

Author Contributions

MH: Conceptualization, Formal Analysis, Investigation, Methodology, Visualization, Writing – original draft, Writing – review & editing. EB: Conceptualization, Investigation, Writing – review & editing. CA: Conceptualization, Investigation, Methodology, Resources, Writing – review & editing. MA: Formal Analysis, Methodology, Writing – review & editing. SK: Conceptualization, Funding acquisition, Investigation, Supervision, Writing – Review & Editing.

Competing Interests

The contact author has declared that none of the authors have any competing interests.

Acknowledgements

This research was supported by the Ocean Frontier Institute (OFI), Natural Sciences and Engineering Research Council of Canada (NSERC), Nova Scotia Graduate Scholarship (NSGS). The authors would like to thank the crew of the Connor's Diving Ltd. vessel EASTCOM, Laura deGelleke, Richard Cheel, Subhadeep Rakshit, and Adam White for assistance in the field. We thank the Bedford Institute of Oceanography for maintaining the timeseries station at the Bedford Basin and making the data

https://doi.org/10.5194/egusphere-2025-2493
Preprint. Discussion started: 17 June 2025

accessible. We thank Claire Normandeau (Dalhousie CERC.OCEAN) and Joshua Landis (Dartmouth College) for analytical assistance.

Works Cited

Aller, R. C., & Kirk Cochran, J. (1976). 234Th/238U disequilibrium in near-shore sediment: Particle reworking and diagenetic time scales. *Earth and Planetary Science Letters*, *29*(1), 37–50. https://doi.org/10.1016/0012-821X(76)90024-8

Amiel, D., & Cochran, J. K. (2008). Terrestrial and marine POC fluxes derived from^{234} Th distributions and δ^{13} C measurements on the Mackenzie Shelf. *Journal of Geophysical Research: Oceans*, *113*(C3), 2007JC004260. https://doi.org/10.1029/2007JC004260

Azetsu-Scott, K., & Johnson, B. D. (1994). Time series of the vertical distribution of particles during and after a spring phytoplankton bloom in a coastal basin. *Continental Shelf Research*, *14*(6), 687–705. https://doi.org/10.1016/0278-4343(94)90113-9

Baskaran, M., Swarzenski, P. W., & Porcelli, D. (2003). Role of colloidal material in the removal of 234Th in the Canada basin of the Arctic Ocean. *Deep Sea Research Part I: Oceanographic Research Papers*, *50*(10–11), 1353–1373. https://doi.org/10.1016/S0967-0637(03)00140-7

Bhat, S. G., Kp, S., & Lal, D. (n.d.). *EARTH AND PLANETARYSCIENCELETTERS 5 (1969) 483-491. NOP,TII-IIOLLAND PUBLISIIINGCO~.IP..AMS'I'ERDA~,I.*

Black, E. E., Algar, C. K., Armstrong, M., & Kienast, S. S. (2023). Insights into constraining coastal carbon export from radioisotopes. *Frontiers in Marine Science*, *10*, 1254316. https://doi.org/10.3389/fmars.2023.1254316

Boetius, A., Albrecht, S., Bakker, K., Bienhold, C., Felden, J., Fernández-Méndez, M., Hendricks, S., Katlein, C., Lalande, C., Krumpen, T., Nicolaus, M., Peeken, I., Rabe, B., Rogacheva, A., Rybakova, E., Somavilla, R., Wenzhöfer, F., & RV Polarstern ARK27-3-Shipboard Science Party. (2013). Export of Algal Biomass from the Melting Arctic Sea Ice. *Science*, *339*(6126), 1430–1432. https://doi.org/10.1126/science.1231346

Bolaños, L. M., Karp-Boss, L., Choi, C. J., Worden, A. Z., Graff, J. R., Haëntjens, N., Chase, A. P., Della Penna, A., Gaube, P., Morison, F., Menden-Deuer, S., Westberry, T. K., O'Malley, R. T., Boss, E., Behrenfeld, M. J., & Giovannoni, S. J. (2020). Small phytoplankton dominate western North Atlantic biomass. *The ISME Journal*, *14*(7), 1663–1674. https://doi.org/10.1038/s41396-020-0636-0

B.T. Hargrave, G.A. Phillips, & S. Taguchi. (1976). *Sedimentation measurements in Bedford Basin, 1973-74*. Fish. Mar. Ser. Res. Dev. Rep. https://doi.org/10.13140/2.1.2815.3125

Buesseler, K. O. (1998). The decoupling of production and particulate export in the surface ocean. *Global Biogeochemical Cycles*, *12*(2), 297–310. https://doi.org/10.1029/97GB03366

Buesseler, K. O., Andrews, J. A., Hartman, M. C., Belastock, R., & Chai, F. (1995). Regional estimates of the export flux of particulate organic carbon derived from thorium-234 during the JGOFS EqPac program. *Deep Sea Research Part II: Topical Studies in Oceanography*, *42*(2–3), 777–804. https://doi.org/10.1016/0967-0645(95)00043-P

Buesseler, K. O., Antia, A. N., Chen, M., Fowler, S. W., Gardner, W. D., Gustafsson, O., Harada, K., Michaels, A. F., Rutgers Van Der Loeff, M., Sarin, M., Steinberg, D. K., & Trull, T. (2007). An assessment of the use of sediment traps for estimating upper ocean particle fluxes. *Journal of Marine Research*, *65*(3), 345–416. https://doi.org/10.1357/002224007781567621

Buesseler, K. O., Benitez-Nelson, C. R., Moran, S. B., Burd, A., Charette, M., Cochran, J. K., Coppola, L., Fisher, N. S., Fowler, S. W., Gardner, W. D., Guo, L. D., Gustafsson, Ö., Lamborg, C., Masque, P., Miquel, J. C., Passow, U., Santschi, P. H., Savoye,

https://doi.org/10.5194/egusphere-2025-2493
Preprint. Discussion started: 17 June 2025

N., Stewart, G., & Trull, T. (2006). An assessment of particulate organic carbon to thorium-234 ratios in the ocean and their impact on the application of 234Th as a POC flux proxy. *Marine Chemistry*, *100*(3–4), 213–233. https://doi.org/10.1016/j.marchem.2005.10.013

Buesseler, K. O., & Boyd, P. W. (2009). Shedding light on processes that control particle export and flux attenuation in the twilight zone of the open ocean. *Limnology and Oceanography*, *54*(4), 1210–1232. https://doi.org/10.4319/lo.2009.54.4.1210

Buesseler, K. O., Lamborg, C. H., Boyd, P. W., Lam, P. J., Trull, T. W., Bidigare, R. R., Bishop, J. K. B., Casciotti, K. L., Dehairs, F., Elskens, M., Honda, M., Karl, D. M., Siegel, D. A., Silver, M. W., Steinberg, D. K., Valdes, J., Van Mooy, B., & Wilson, S. (2007). Revisiting Carbon Flux Through the Ocean's Twilight Zone. *Science*, *316*(5824), 567–570. https://doi.org/10.1126/science.1137959

Buesseler, K. O., Livingston, H. D., Cochran, Kirk, & Bacon, Micheal. (1992). *Carbon and nitrogen export during the JGOFS North Atlantic Bloom Experiment estimated from 234Th:23aU disequilibria*.

Burt, W. J., Thomas, H., Fennel, K., & Horne, E. (2013). Sediment-water column fluxes of carbon, oxygen and nutrients in Bedford Basin, Nova Scotia, inferred from^{224} Ra measurements. *Biogeosciences*, *10*(1), 53–66. https://doi.org/10.5194/bg-10-53-2013

Butman, C. A. (1989). Sediment-trap experiments on the importance of hydrodynamical processes in distributing settling invertebrate larvae in near-bottom waters. *Journal of Experimental Marine Biology and Ecology*, *134*(1), 37–88. https://doi.org/10.1016/0022-0981(90)90055-H

Cai, P., Dai, M., Lv, D., & Chen, W. (2006). An improvement in the small-volume technique for determining thorium-234 in seawater. *Marine Chemistry*, *100*(3–4), 282–288. https://doi.org/10.1016/j.marchem.2005.10.016

Ceballos-Romero, E., Buesseler, K. O., & Villa-Alfageme, M. (2022). Revisiting five decades of^{234} Th data: A comprehensive global oceanic compilation. *Earth System Science Data*, *14*(6), 2639–2679. https://doi.org/10.5194/essd-14-2639-2022

Charette, M. A., & Moran, S. B. (1999). Rates of particle scavenging and particulate organic carbon export estimated using 234Th as a tracer in the subtropical and equatorial Atlantic Ocean. *Deep Sea Research Part II: Topical Studies in Oceanography*, *46*(5), 885–906. https://doi.org/10.1016/S0967-0645(99)00006-5

Charette, M. A., Moran, S. B., Pike, S. M., & Smith, J. N. (2001). Investigating the carbon cycle in the Gulf of Maine using the natural tracer thorium 234. *Journal of Geophysical Research: Oceans*, *106*(C6), 11553–11579. https://doi.org/10.1029/1999JC000277

Clevenger, S. J., Benitez-Nelson, C. R., Drysdale, J., Pike, S., Puigcorbé, V., & Buesseler, K. O. (2021). Review of the analysis of 234Th in small volume (2–4 L) seawater samples: Improvements and recommendations. *Journal of Radioanalytical and Nuclear Chemistry*, *329*(1), 1–13. https://doi.org/10.1007/s10967-021-07772-2

Coale, K. H., & Bruland, K. W. (1985). ^{234} Th:^{238} U disequilibria within the California Current1. *Limnology and Oceanography*, *30*(1), 22–33. https://doi.org/10.4319/lo.1985.30.1.0022

Cochran, J. K., Barnes, C., Achman, D., & Hirschberg, D. J. (1995). Thorium-234/uranium-238 disequilibrium as an indicator of scavenging rates and participate organic carbon fluxes in the Northeast Water Polynya, Greenland. *Journal of Geophysical Research: Oceans*, *100*(C3), 4399–4410. https://doi.org/10.1029/94JC01954

[Dataset]. (n.d.). [Dataset].

Environment and Climate Change Canada. (2018). *Historical climate data: Halifax International Airport* [Dataset]. https://climate.weather.gc.ca/historical_data/search_historic_data_stations_e.html?StationID=50620&Month=8&Day=1&Year=2018&timeframe=2&StartYear=1840&EndYear=2018&searchType=stnProx&txtRadius=25&optProxType=navLink&txtLatDe

cDeg=44.881111111111&txtLongDecDeg=63.508611111111&optLimit=specDate&selRowPerPage=25&station=HALIFAX+INTL+A

Evangeliou, N., Florou, H., & Scoullos, M. (2011). POC and particulate 234Th export fluxes estimated using 234Th/238U disequilibrium in an enclosed Eastern Mediterranean region (Saronikos Gulf and Elefsis Bay, Greece) in seasonal scale. *Geochimica et Cosmochimica Acta*, *75*(19), 5367–5388. https://doi.org/10.1016/j.gca.2011.04.005

Fader, G. B. J., & Miller, R. O. (2008). *Surficial geology, Halifax Harbour, Nova Scotia* (p. 590). Natural Resources Canada. https://doi.org/10.4095/224797

Falkowski, P. G., Flagg, C. N., Rowe, G. T., Smith, S. L., Whitledge, T. E., & Wirick, C. D. (1988). The fate of a spring phytoplankton bloom: Export or oxidation? *Continental Shelf Research*, *8*(5–7), 457–484. https://doi.org/10.1016/0278-4343(88)90064-7

Faust, J. C., & Knies, J. (2019). Organic Matter Sources in North Atlantic Fjord Sediments. *Geochemistry, Geophysics, Geosystems*, *20*(6), 2872–2885. https://doi.org/10.1029/2019GC008382

Forster, S., Turnewitsch, R., Powilleit, M., Werk, S., Peine, F., Ziervogel, K., & Kersten, M. (2009). Thorium-234 derived information on particle residence times and sediment deposition in shallow waters of the south-western Baltic Sea. *Journal of Marine Systems*, *75*(3–4), 360–370. https://doi.org/10.1016/j.jmarsys.2008.04.004

Foster, J. M., & Shimmield, G. B. (2002). 234Th as a tracer of particle flux and POC export in the northern North Sea during a coccolithophore bloom. *Deep Sea Research Part II: Topical Studies in Oceanography*, *49*(15), 2965–2977. https://doi.org/10.1016/S0967-0645(02)00066-8

GEBCO Compilation Group. (2022). *GEBCO 2022 Grid* [Dataset]. https://doi.org/10.5285/c6612cbe-50b3-0cff-e053-6c86abc040b9

Graff, J. R., Nelson, N. B., Roca-Martí, M., Romanelli, E., Kramer, S. J., Erickson, Z., Cetinić, I., Buesseler, K. O., Passow, U., Zhang, X., Benitez-Nelson, C., Bisson, K., Close, H. G., Crockford, T., Fox, J., Halewood, S., Lam, P., Roesler, C., Sweet, J., … Siegel, D. A. (2023). Reconciliation of total particulate organic carbon and nitrogen measurements determined using contrasting methods in the North Pacific Ocean as part of the NASA EXPORTS field campaign. *Elem Sci Anth*, *11*(1), 00112. https://doi.org/10.1525/elementa.2022.00112

Haas, S., Robicheau, B. M., Rakshit, S., Tolman, J., Algar, C. K., LaRoche, J., & Wallace, D. W. R. (2021). Physical mixing in coastal waters controls and decouples nitrification via biomass dilution. *Proceedings of the National Academy of Sciences*, *118*(18), e2004877118. https://doi.org/10.1073/pnas.2004877118

Hung, C.-C., Gong, G.-C., & Santschi, P. H. (2012). 234Th in different size classes of sediment trap collected particles from the Northwestern Pacific Ocean. *Geochimica et Cosmochimica Acta*, *91*, 60–74. https://doi.org/10.1016/j.gca.2012.05.017

Kepkay, Niven, S.E.H, & Jellett J.F. (1997). Colloidal organic carbon and phytoplankton speciation during a coastal bloom. *Journal of Plankton Research*, *19*(3), 369–389. https://doi.org/10.1093/plankt/19.3.369

Lalande, C., Moran, S. B., Wassmann, P., Grebmeier, J. M., & Cooper, L. W. (2008). 234Th-derived particulate organic carbon fluxes in the northern Barents Sea with comparison to drifting sediment trap fluxes. *Journal of Marine Systems*, *73*(1–2), 103–113. https://doi.org/10.1016/j.jmarsys.2007.09.004

Lam, P. J., Ohnemus, D. C., & Auro, M. E. (2015). Size-fractionated major particle composition and concentrations from the US GEOTRACES North Atlantic Zonal Transect. *Deep Sea Research Part II: Topical Studies in Oceanography*, *116*, 303–320. https://doi.org/10.1016/j.dsr2.2014.11.020

Lampitt, R. S. (1985). Evidence for the seasonal deposition of detritus to the deep-sea floor and its subsequent resuspension. *Deep Sea Research Part A. Oceanographic Research Papers*, *32*(8), 885–897. https://doi.org/10.1016/0198-0149(85)90034-2

Lepore, K., Moran, S. B., Grebmeier, J. M., Cooper, L. W., Lalande, C., Maslowski, W., Hill, V., Bates, N. R., Hansell, D. A., Mathis, J. T., & Kelly, R. P. (2007). Seasonal and interannual changes in particulate organic carbon export and deposition in the Chukchi Sea. *Journal of Geophysical Research: Oceans*, *112*(C10), 2006JC003555. https://doi.org/10.1029/2006JC003555

Li, W. K. W., & Glen Harrison, W. (2008). Propagation of an atmospheric climate signal to phytoplankton in a small marine basin. *Limnology and Oceanography*, *53*(5), 1734–1745. https://doi.org/10.4319/lo.2008.53.5.1734

Lin, W., Chen, L., Zeng, S., Li, T., Wang, Y., & Yu, K. (2016). Residual β activity of particulate 234Th as a novel proxy for tracking sediment resuspension in the ocean. *Scientific Reports*, *6*(1), 27069. https://doi.org/10.1038/srep27069

Longhurst, A., Sathyendranath, S., Platt, T., & Caverhill, C. (1995). An estimate of global primary production in the ocean from satellite radiometer data. *Journal of Plankton Research*, *17*(6), 1245–1271. https://doi.org/10.1093/plankt/17.6.1245

Luo, Y., Miller, L. A., De Baere, B., Soon, M., & Francois, R. (2014). POC fluxes measured by sediment traps and 234Th:238U disequilibrium in Saanich Inlet, British Columbia. *Marine Chemistry*, *162*, 19–29. https://doi.org/10.1016/j.marchem.2014.03.001

Martin, J. H., Knauer, G. A., Karl, D. M., & Broenkow, W. W. (1987). VERTEX: Carbon cycling in the northeast Pacific. *Deep Sea Research Part A. Oceanographic Research Papers*, *34*(2), 267–285. https://doi.org/10.1016/0198-0149(87)90086-0

Muller-Karger, F. E., Varela, R., Thunell, R., Luerssen, R., Hu, C., & Walsh, J. J. (2005). The importance of continental margins in the global carbon cycle. *Geophysical Research Letters*, *32*(1), 2004GL021346. https://doi.org/10.1029/2004GL021346

Owens, S. A., Buesseler, K. O., & Sims, K. W. W. (2011). Re-evaluating the 238U-salinity relationship in seawater: Implications for the 238U–234Th disequilibrium method. *Marine Chemistry*, *127*(1–4), 31–39. https://doi.org/10.1016/j.marchem.2011.07.005

Owens, S. A., Pike, S., & Buesseler, K. O. (2015). Thorium-234 as a tracer of particle dynamics and upper ocean export in the Atlantic Ocean. *Deep Sea Research Part II: Topical Studies in Oceanography*, *116*, 42–59. https://doi.org/10.1016/j.dsr2.2014.11.010

Platt, T. (n.d.). *ANALYSIS OF THE IMPORTANCE OF SPATIAL AND TEMPORAL HETEROGENEITY JN THE ESTIMATION OF ANNUAL PRODUCTION BY PHYTOPLANKTON IN A SMALL, ENRICHED, MARINE BASIN*.

Puigcorbé, V., Masqué, P., & Le Moigne, F. A. C. (2020). Global database of ratios of particulate organic carbon to thorium-234 in the ocean: Improving estimates of the biological carbon pump. *Earth System Science Data*, *12*(2), 1267–1285. https://doi.org/10.5194/essd-12-1267-2020

Rakshit, S., Dale, A. W., Wallace, D. W., & Algar, C. K. (2023). Sources and sinks of bottom water oxygen in a seasonally hypoxic fjord. *Frontiers in Marine Science*, *10*, 1148091. https://doi.org/10.3389/fmars.2023.1148091

Rakshit, S., Glock, N., Dale, A. W., Armstrong, M. M. L., Scholz, F., Mutzberg, A., & Algar, C. K. (2025). Foraminiferal denitrification and deep bioirrigation influence benthic biogeochemical cycling in a seasonally hypoxic fjord. *Geochimica et Cosmochimica Acta*, *388*, 268–282. https://doi.org/10.1016/j.gca.2024.10.010

Robicheau, B. M., Tolman, J., Bertrand, E. M., & LaRoche, J. (2022). Highly-resolved interannual phytoplankton community dynamics of the coastal Northwest Atlantic. *ISME Communications*, *2*(1), 38. https://doi.org/10.1038/s43705-022-00119-2

Shan, S., Sheng, J., Thompson, K. R., & Greenberg, D. A. (2011). Simulating the three-dimensional circulation and hydrography of Halifax Harbour using a multi-nested coastal ocean circulation model. *Ocean Dynamics*, *61*(7), 951–976. https://doi.org/10.1007/s10236-011-0398-3

Shi, Q., & Wallace, D. (2018). A 3-year time series of volatile organic iodocarbons in Bedford Basin, Nova Scotia: A northwestern Atlantic fjord. *Ocean Science*, *14*(6), 1385–1403. https://doi.org/10.5194/os-14-1385-2018

https://doi.org/10.5194/egusphere-2025-2493
Preprint. Discussion started: 17 June 2025

Siegel, D. A., Buesseler, K. O., Doney, S. C., Sailley, S. F., Behrenfeld, M. J., & Boyd, P. W. (2014). Global assessment of ocean carbon export by combining satellite observations and food-web models. *Global Biogeochemical Cycles*, *28*(3), 181–196. https://doi.org/10.1002/2013GB004743

Trimble, S. M., & Baskaran, M. (2005). The role of suspended particulate matter in 234Th scavenging and 234Th-derived export fluxes of POC in the Canada Basin of the Arctic Ocean. *Marine Chemistry*, *96*(1–2), 1–19. https://doi.org/10.1016/j.marchem.2004.10.003

Wassmann, P. (1984). Sedimentation and benthic mineralization of organic detritus in a Norwegian fjord. *Marine Biology*, *83*(1), 83–94. https://doi.org/10.1007/BF00393088

Wei, C.-L., & Murray, J. W. (1992). Temporal variations of^{234} Th activity in the water column of Dabob Bay: Particle scavenging. *Limnology and Oceanography*, *37*(2), 296–314. https://doi.org/10.4319/lo.1992.37.2.0296

Yang, W., Tian, J., Chen, M., Zheng, M., & Chen, M. (2022). A New Radiotracer for Particulate Carbon Dynamics: Examination of^{210} Bi-^{210} Pb in Seawater. *Geochemistry, Geophysics, Geosystems*, *23*(12), e2022GC010656. https://doi.org/10.1029/2022GC010656